The effect of specimen size on the unconfined compressive strength of cement-stabilized granular mixtures made of natural and recycled aggregates

Taylor & Francis
Taylor & Francis Group

Road Materials and Pavement Design

THE EFFECT OF SPECIMEN SIZE ON THE UNCONFINED COMPRESSIVE STRENGTH OF CEMENT-STABILIZED GRANULAR MIXTURES MADE OF NATURAL AND RECYCLED AGGREGATES

Submission ID	244659365
Article Type	Research Article
Keywords	unconfined compressive strength, cement-stabilized granular material, construction and demolition waste aggregate, slenderness, loading modes
Authors	Luca Tefa, Alessandro Corradini, Arastoo Karimi, Gianluca Cerni, Marco Bassani

THE EFFECT OF SPECIMEN SIZE ON THE UNCONFINED COMPRESSIVE STRENGTH OF CEMENT-STABILIZED GRANULAR MIXTURES MADE OF NATURAL AND RECYCLED AGGREGATES

Luca TEFA[1,*], Alessandro CORRADINI[2], Arastoo KARIMI[1], Gianluca CERNI[2], Marco BASSANI[1]

[1] Department of Environment, Land and Infrastructure Engineering, Politecnico di Torino, Torino, Italy

[2] Department of Civil and Environmental Engineering, University of Perugia, Perugia, Italy

* corresponding author

Luca Tefa: luca.tefa@polito.it

Alessandro Corradini: alessandro.corradini@unipg.it

Arastoo Karimi: arastoo.karimi@polito.it

Gianluca Cerni: gianluca.cerni@unipg.it

Marco Bassani: marco.bassani@polito.it

ABSTRACT

The cement-stabilization technique is employed on natural and recycled granular materials to improve their mechanical properties and durability. The strength of cement-stabilized granular materials is assessed by the unconfined compressive strength on laboratory compacted specimens typically after 7 days of curing. Standards and technical specifications establish specimen height and diameter and loading mode (i.e., control of displacement or force). The challenge of comparing the strength of different mixtures or assessing material strength within the acceptance limits of technical specifications is exacerbated by the heterogeneity of standards.

This research investigates the effect of specimen size on the unconfined compressive strength of cement-stabilized granular materials by varying the height and diameter. Two types of aggregate, natural and recycled from construction and demolition waste, were investigated. The study also investigated the impact of the loading mode application on the strength. The results revealed significant differences in strength due to variations in specimen size and loading mode for both mixtures. As expected, an increase in specimen slenderness resulted in a decrease in compressive strength. The loading mode also affects strength, with controlled-displacement loading providing higher strengths. A linear regression model was developed to quantify the effect of specimen size and loading mode on the compressive strength of the two cement-stabilized materials. Based on this model, tables of conversion factors are provided to facilitate the comparison and conversion of strength data.

KEYWORDS: unconfined compressive strength; cement-stabilized granular material; construction and demolition waste aggregate; slenderness; loading modes.

1. INTRODUCTION

Cement-stabilized granular mixtures (CSGMs) are blends of aggregates, cement, and water. Cement is typically added in the range of 2-4% of the aggregate mass (Maher & Ho, 1993; Mohammad et al., 2000). The cement-stabilization technique is used to improve the mechanical properties and durability of granular materials when additional stiffness to bear traffic loads is required for base and subbase pavement layers (Yoder & Witczak, 1975).

To ensure adequate performance, technical standards establish minimum requirements for aggregate properties (fragmentation resistance, soundness, shape and flakiness, freeze/thaw resistance, alkali-silica reaction, plasticity, etc.) (Centro Sperimentale Interuniversitario di Ricerca Stradale, 2001; Federal Highway Administration Research and Technology, 2016). Additionally, they mandate the use of cement classified according to the harmonized standard EN 197-1 (European Committee for Standardization, 2011). At the same time, some technical specifications indicate the aggregate blend gradations depending on the pavement type (flexible or rigid) and the layer in which the CSGM is laid (Lotfi & Witczak, 1981; Halsted et al., 2006; European Committee for Standardization, 2013b; Federal Highway Administration Research and Technology, 2016). The CSGM strength is evaluated through indirect tensile and unconfined compressive strength (UCS) tests on laboratory-compacted specimens after 7 days of curing. These two strengths are also used on in quality assurance procedures to determine whether the material is suitable for a specific construction task (Biswal et al., 2020). For instance, the Mechanistical-Empirical Pavement Design Guide method requires a minimum UCS of 5.2 MPa (750 psi) and 1.7 MPa (250 psi) at 7 days of curing for base and subbase layers respectively (Department of the Army & Department of the Air Force, 1994; Applied Research Associates Inc., 2004). The Italian technical specifications (Centro Sperimentale Interuniversitario di Ricerca Stradale, 2001) prescribes that the UCS at 7-days of curing should be in the 2.5-4.5 MPa range.

Although UCS is a widely used and relatively simple testing procedure for the inspection and approval of CSGMs, current standards and specifications differ based on the specimen formation procedure, i.e., the compaction method and the sample size (H = height, D = diameter, or H/D ratio). In fact, technical specifications have been updated to address these differences. In European technical standards, EN 13286-41 (European Committee for Standardization, 2021) maintains different procedures for CSGM. The standard allows for broad requirements regarding sample shape, size, and compaction methods Specific sample sizes are set based on compaction method and maximum grain size (D_g) in the mixture in accordance with EN 13286-50 (European Committee for Standardization, 2004d), EN 13286-51 (European Committee for Standardization, 2004a), EN 13286-52 (European Committee for Standardization, 2004b), and EN 13286-53 (European Committee for Standardization, 2004c). Therefore, any variation in these testing parameters leads to different outcomes, which cannot be compared to each other. Table 1 summarizes the most common technical standards for UCS testing including different sample sizes and preparation methods. It is worth noting that some authors perform tests on CSGMs by referring to standards conceived for different material types.

Table 1 – Summary of standards for UCS test on cylindrical specimens (Note: D = diameter; H = height; CD = constant displacement; CF = constant force; P_{19mm} = passing at 19 mm sieve; $P_{4.75mm}$ = passing at 4.75 mm sieve; D_g= grain maximum diameter)

Standard for testing	Mixtures	Loading method	Standard for sample preparation	Specimen size (D; H) in mm	References
EN 13286-41	Hydraulically bound mixtures	CF to obtain failure in 30-120 s interval	EN 13286-50 (Proctor)	(100; 120) if D_g < 22.4 mm (150; 120) if D_g < 31.5 mm	(European Committee for Standardization, 2021), (European Committee for Standardization, 2004c)
			EN 13286-51 (vibrating hammer)	(100; 100) if D_g < 22.4 mm (150; 150) if D_g < 31.5 mm	
			EN 13286-52 (vibro-compression)	(100; 100) or (100; 200) if D_g < 22.4 mm (160; 160) or (160; 320) if D_g < 31.5 mm	
			EN 13286-53 (axial compression)	(50; 50) or (50; 100) if D_g < 11.2 mm (100; 100) or (100; 200) if D_g < 22.4 mm	
ASTM D 5102	Soil-lime mixtures	CD 0.5-2.0% strain/min	Method A: Pressing, kneading or impact action	H/D between 2 and 2.5	(American Society for Testing and Materials, 2009; American Society for Testing and Materials, 2012)
			Method B: ASTM D 698	(101.6; 116.4)	
ASTM D 1633	Soil-cement mixtures	CD 1 mm/min	Method A: ASTM D 698 if P_{19mm} > 30%	(101.6; 116.4)	(American Society for Testing and Materials, 2007; American Society for Testing and Materials, 2012)
			Method B: ASTM D 698 if $P_{4.75mm}$ =100	(71.1;142.2)	

For instance, Mohammadinia et al., (2014) performed UCS tests on recycled CSGMs as per ASTM 5102 (American Society for Testing and Materials, 2009) albeit this standard was conceived for soil-lime mixtures. In accordance with this standard, two cylindrical specimens with a minimum diameter of 50 mm with (i) H/D ratio between 2.0 and 2.5 or (ii) H/D = 1.15 can undergo UCS tests depending on the compaction method. Meanwhile, the ASTM D 1633 (American Society for Testing and Materials, 2007) for soil-cement mixtures considers (i) a H/D ratio equal to 1.15 and 101.6 mm (4.0 in.) in diameter and 116.4 mm (4.6 in.) in height for materials with a retained at 19 mm sieve lower than 30%, and (ii) a H/D = 2.0 and 71.1 mm (2.8 in.) in diameter and 142.2 mm (5.6 in.) in height for aggregate passing the 4.75 mm sieve. When the loading mode is the concern, the EN 13286-41 (European Committee for Standardization, 2021) advocates the application of a constant force (CF) to achieve a specimen failure in the 30 to 120 s range. ASTM 5102 (American Society for Testing and Materials, 2009) and ASTM D 1633 (American Society for Testing and Materials, 2007) prescribe a UCS test by applying a constant displacement (CD) rate (Table 1).

Based on the context provided, it is evident that current requirements for the UCS of CSGMs (The British Standards Institution, 2018; Rashidi & Ashtiani, 2019) prevent the comparison of UCS outcomes with the acceptance threshold of technical specifications and make it difficult to interpret the results from different studies. Therefore, in this research we investigated the effects of the specimen size (H, D, and H/D ratio) on UCS. Two CSGMs, one containing natural and the other containing recycled aggregates from construction and demolition waste (CDW), were evaluated for their influence on UCS under two loading application modes: controlled force and displacement rate.

Specimens of 55, 100, 150, and 200 mm in height with a diameter of 100 mm, and specimens of 100, 150, and 200 mm in height and a diameter 150 mm were prepared in the 0.55-2.00 H/D ratio range. Five replicates per the sample set were produced to strengthen the statistical validity of the results. To exclude any

secondary effects, the same type and quantity of cement (3% wt. of dry aggregate), and particle size distribution for both natural and recycled aggregates were adopted.

2. MATERIALS AND METHODS

2.1 Materials

Natural (NAT) and CDW recycled aggregates were obtained from Spinelli & Mannocchi Srl (Lidarno, Perugia, Italy) and Cavit SpA (La Loggia, Turin, Italy), respectively, while the cement was provided by Italcementi Srl. Both the natural and recycled granular materials were divided into size fractions of (mm-mm) 20-16, 16-8, 8-4, 4-2, 2-1, 1-0.5, 0.5-0.125, 0.125-0.063, and < 0.063 mm. Each aggregate blend was obtained by recombing the size classes according to Italian specification (Centro Sperimentale Interuniversitario di Ricerca Stradale, 2001), and adjusting for the maximum grain size of 20 mm as shown in Figure 1.

The oven-dried particle density of the NAT and CDW aggregate samples were deemed to be 2691 and 2597 kg/m^3 respectively as per EN 1097-6 (European Committee for Standardization, 2013a). Moreover, the 4-20 mm fraction of CDW aggregate was classified according to the constituents reported in EN 933-11 (European Committee for Standardization, 2009). The composition obtained consisted of 22.1% of *Rc* (concrete and mortar), 51.7% of *Ru* (unbound aggregate and natural stone), 10.6% *Rb* (clay masonry particles), 15.4% *Ra* (bituminous materials), and 0.2% of impurities (non-floating wood, plastic, etc.).

A CEM-III/A 42.5 N blast furnace cement (35-64% clinker and 36-65% blast furnace slag) in accordance with EN 197-1 (European Committee for Standardization, 2011) was used. A cement quantity of 3% was used for both the natural and recycled aggregate mixtures, which falls within the typical range of 2-5% of the dry aggregate mass (Lotfi & Witczak, 1981; Xuan et al., 2012; Bassani et al., 2017).

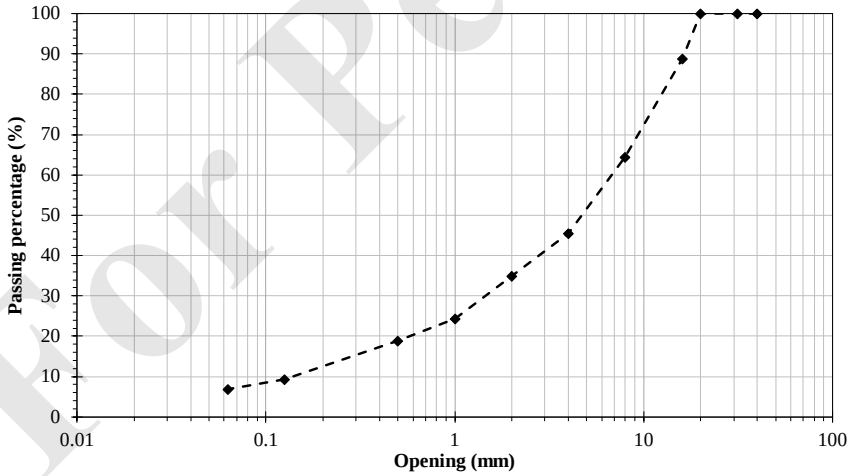

Figure 1 – Reference particle size distribution curve for CSGM from (Centro Sperimentale Interuniversitario di Ricerca Stradale, 2001). The grain size distribution curve shows 100% passing at 20 mm, 88.9% at 16 mm, 64.4% at 8 mm, 45.6% at 4 mm, 35.0% at 2 mm, 24.3% at 1.0 mm, 19.0% at 0.5 mm, 9.3% at 0.125 mm, and 6.9% at 0.063 mm.

2.2 Specimen preparation and testing

A modified Proctor compaction test (five layers, 56 blows each, 4.5 kg hammer dropped from 45.7 cm) was conducted to establish the optimum moisture content (OMC) that would maximize the dry density (MDD) of both the natural and recycled CSGMs according to the EN 13286-2 (European Committee for Standardization, 2010). The cement was mixed thoroughly with the aggregate blends prior to the samples being compacted. As shown in Figure 2, the recycled CSGM required a significantly higher OMC to achieve the MDD compared to the natural one due to the presence of porosity in bricks, tiles, and concrete particles that absorb more moisture than natural aggregates. The OMC and MDD values determined for natural and recycled CSGMs were (4.6%; 2.298 Mg/m^3) and (9.3%; 2.083 Mg/m^3), respectively.

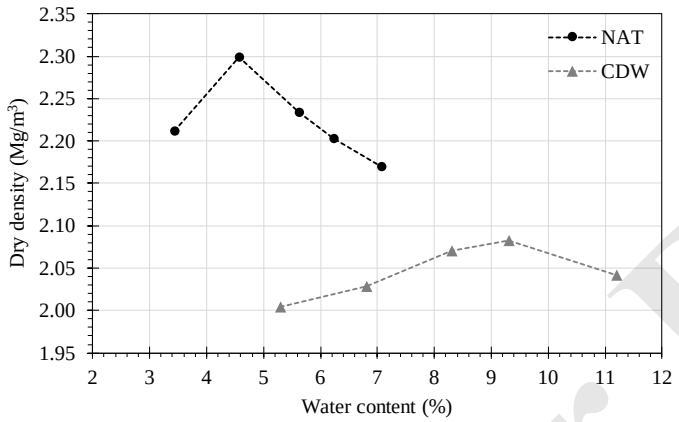

Figure 2 – Proctor compaction curves for natural and recycled (CDW) CSGM.

Specimens were prepared by first mixing aggregates and water (at the OMC) and then adding cement after 24 h in a humidity-controlled environment. Cylindrical specimens were compacted using a gyratory shear compactor in accordance with previous investigations (Autelitano & Giuliani, 2016; Bassani et al., 2017). Figure 3 illustrates the different specimen sizes with D equal to 100 mm (H = 55-, 100-, 150-, and 200-mm) and 150 mm (H = 100-, 150-, and 200-mm). The specimens were compacted in one or more layers, depending on the final height (Figure 3), to ensure uniform distribution of compaction energy throughout the specimen height. The first layer was always set at the minimum height possible for compaction using the gyratory compaction equipment of 55 mm. To control the dry density of specimens, the following parameters were applied: a vertical pressure of 600 kPa, a tilting mould angle of 1.25°, a rotation speed of 30 rpm, and a fixed number of gyrations equal to 40 and 50 for natural and recycled CSGM respectively. The number of gyrations was determined via a preliminary investigation involving multiple trials. During these trials, the optimal number of gyrations required to achieve the desired specimen height for both cement-stabilized NAT and CDW aggregate blends was determined.

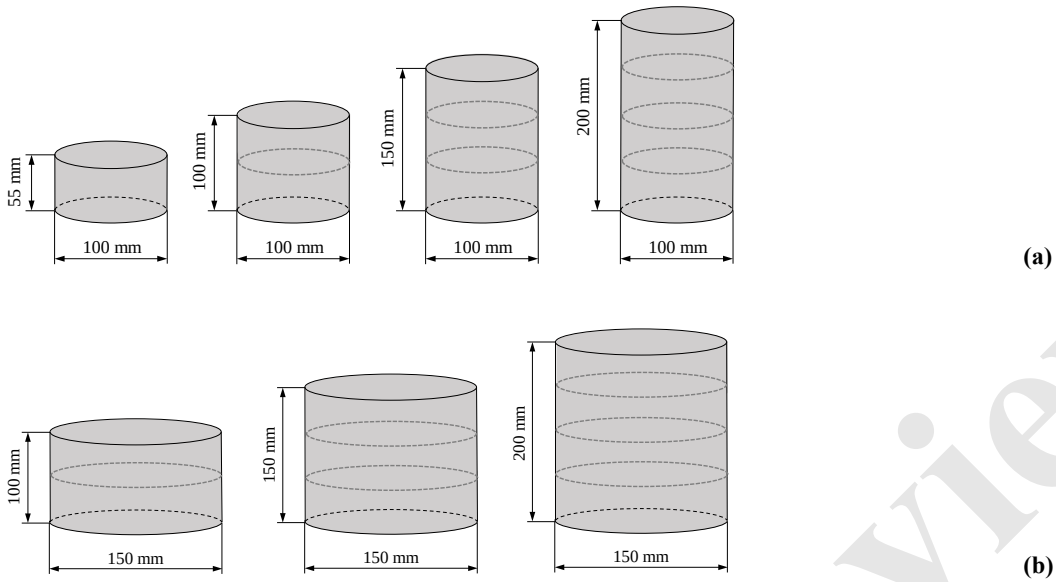

Figure 3 – Scheme of the different specimen sizes: (a) 100 mm diameter, (b) 150 mm diameter.

After compaction, specimens were cured at room temperature (20 °C) and relative humidity higher than 90% for 7 days. UCS tests were carried out by means of a 200-kN testing device able to carry out tests at (i) the constant displacement (CD) rate of 0.5 mm/min and (ii) the constant force (CF) by setting a stress of 0.08 MPa/s to ensure test durations fell within the 30-120 s range in compliance with EN 13286-41 (European Committee for Standardization, 2021).

2.3 Statistical analyses

A multiple linear regression model was used to predict the evolution of USC. The choice stems from the continuous and normally distributed nature of the variables under examination. Multiple linear regression offers simplicity and efficiency and facilitates the clear interpretation and reliable generalization of results. Its built-in hypothesis testing capabilities enhance the reliability of analyses, making it a robust method across diverse research domains (Wooldridge, 2019). The general form of the multiple linear regression model is presented by Eq. 1:

$$Y = \beta_0 + \beta_1 X_1 + \beta_2 X_2 + \ldots + \beta_n X_n + \varepsilon \qquad \textbf{eq. 1}$$

where β_0 is the constant coefficient of the model and $\beta_1, \ldots, \beta_K$ are the slope coefficients for the independent variables $X_1, \ldots, X_n$. The ordinary least square (OLS) method will be used to estimate the model coefficients. The variables may exhibit various functional forms, such as logarithmic or quadratic expressions. The STATA statistical software, Version 17 (StataCorp, 2021) was used for statistical analyses and modelling.

To ensure that the Ordinary Least Squares (OLS) method serves as the best linear unbiased estimator (BLUE), it is essential that the assumptions underlying the classic linear regression model have been verified. To this end, various statistical tests have been applied including Ramsey's RESET test (Ramsey, 1969) which

was employed to evaluate potential model misspecification by identifying whether any significant variables were excluded from the model. Following the evaluation of model specification, the heteroscedasticity test was conducted to examine the variance of response results across different levels of the independent variables. The Breusch-Pagan test (Breusch & Pagan, 1979) was used to detect the presence of heteroscedasticity within the proposed model, serving as a crucial step in validating its assumptions and efficacy. In multiple regression models, multicollinearity occurs when independent variables are highly intercorrelated, with no definitive acceptance threshold. A model is considered more robust when it features lower inter-variable correlations. The Variance Inflation Factor (VIF) is a commonly employed technique to measure the influence of multicollinearity on the variance of regression coefficients. While a lower VIF indicates better conditions for regression analysis, it is generally recommended that the VIF should not exceed a threshold value of 10 (James et al., 2021). Despite the tendency of residuals to approximate a normal distribution in larger sample sizes, we also assessed their normality using a normal probability plot. The model's goodness-of-fit was evaluated by means of the adjusted R-squared and Root Mean Square Error (RMSE) metrics (Wooldridge, 2019).

3. RESULTS

3.1 Density and compressive strength

The average results for dry density are summarized in Figure 4. Considering the CDW aggregate specimens, for D = 100 mm, the average dry density was in the 1.983-2.049 Mg/m³ range, while for D = 150 mm, the dry density was in the 2.037-2.057 Mg/m³ range. Specimens consisting of NAT aggregates showed higher densities than those of CDW aggregates because of the presence of brick and tiles that have a lower density than natural materials (Bassani & Tefa, 2018; Wang et al., 2020; Esfahani, 2020).

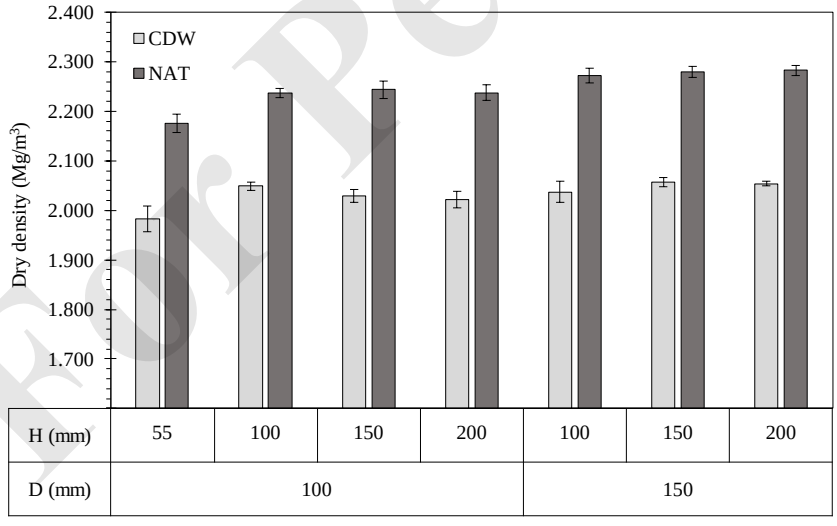

Figure 4 – Average dry densities of CDW and NAT specimens depending on diameter (D) and height (H). The error bars indicate one standard deviation.

In this investigation, this was clearly evidenced when samples were extruded from the moulds, resulting in residual air voids on the sample lateral surface. The smaller the sample, the greater this effect. Therefore, as the diameter of the specimen increases, the wall effect decreases resulting in a denser structure of compacted materials (Olard & Perraton, 2010).

Table 2 lists the average UCS values for various diameters, H/D ratios, loading application modes, and aggregate types. The data were subjected to ANOVA to statistically assess the effect of the experimental variables on the final UCS values. Since the assumption checks for homogeneity of variances (*Levene L* = 4.14, *p*-value < .001) and normal distribution of observations (*Shapiro-Wilk* = 0.968, *p*-value = .003) did not support the hypothesis testing, the ANOVA was performed on *Ln*(*UCS*) values (*Levene L* = 1.50, *p*-value < .084; *Shapiro-Wilk* = 0.994, *p*-value = .820) with a significance level of 5%.

The H/D ratio significantly influences the *Ln*(*UCS*) ($F_{17,5}$ = 936.6, *p*-value < .001). As expected, the H/D ratio increases as the UCS decreases. A statistically significant effect of the loading mode on the UCS ($F_{17,1}$ = 162.4, *p*-value < .001) was also observed. Apart from both the NAT and CDW specimens with D = 150 mm and H/D = 0.67, the UCS results were generally higher for the CD loading mode than they were for the CF one. Considering the condition with H/D = 1, small differences in the average UCS values of Table 2 between 100 mm and 150 mm are evident. Nevertheless, the diameter size did not have a discernible effect on UCS strength. On the other hand, the material type plays a significant role in determining the final UCS ($F_{17,1}$ = 913.2, *p*-value < .001). As expected, the use of NAT aggregates provides higher strength to the cement-stabilized mixtures in comparison to recycled material from CDW in line with previous investigations (Tataranni et al., 2018; Xue et al., 2022).

Table 2 – Average results of UCS in MPa depending on the material (CSGM with natural and recycled aggregates), diameter (D), the H/D ratio, the loading procedure, and the material. The number in the brackets indicate the standard deviation.

D (mm)	H/D ratio	Natural CSGM		CDW CSGM	
		CF	CD	CF	CD
100	0.55	11.19 (± 0.90)	11.90 (± 1.31)	7.77 (± 0.54)	6.80 (± 0.16)
	1.00	6.52 (± 0.31)	7.51 (± 0.51)	3.78 (± 0.50)	4.92 (± 0.32)
	1.50	3.29 (± 0.18)	4.28 (± 0.30)	1.86 (± 0.22)	2.86 (± 0.15)
	2.00	2.09 (± 0.17)	2.89 (± 0.38)	1.66 (± 0.11)	2.30 (± 0.07)
150	0.67	11.95 (± 0.82)	11.39 (± 0.79)	6.53 (± 0.31)	5.96 (± 0.47)
	1.00	5.78 (± 0.56)	7.70 (± 0.53)	4.15 (± 0.29)	4.63 (± 0.29)
	1.33	3.95 (± 0.20)	5.70 (± 0.26)	2.61 (± 0.29)	3.75 (± 0.11)

3.2 Regression analysis

The statistical model for the estimation of UCS was calibrated using the independent variables listed in Table 3. Table 4 presents the Person's r correlation matrix (with *p*-values) between the independent variables investigated and the recorded UCS values. Numerous attempts were made to include or exclude the independent variables from Table 4, while also varying the mathematical function (logarithm, exponential) that describes the behaviour of both dependent and independent factors. The linear regression model's goodness of fit was evaluated using the adjusted coefficient of determination (R^2_{adj}) value.

Table 3 – Definition of Independent variables

Variable	Symbol	Unit	Interval values
Aggregate type	A_{type}	(-)	0 = CDW aggregate 1 = NAT aggregate
Loading configuration	L_c	(-)	0 = CD (constant displacement) 1 = CF (constant force)
Specimen diameter	D	(mm)	100, 150
Specimen height	H	(mm)	55, 100, 150, 200
H/D ratio	$R_{H/D}$	(-)	0.55, 0.67, 1.00, 1.33, 1.50, 2.00
Measured dry density	γ_d	Mg/m^3	Range (1.983; 2.312)
Difference between effective (measured) dry density and the target dry density (i.e., the MDD)	$\gamma_{d,diff}$	Mg/m^3	Range (-0.135; 0.014)

A significant correlation was found between aggregate type (A_{type}) and measured dry density (γ_d), with coefficients of 0.40 and 0.35, respectively at the 95% confidence level. Furthermore, the size-related variables, such as the diameter (D) and height (H) of the sample, had a significant impact at the 95% confidence level. The H/D ratio shows a statistically significant correlation and may improve the prediction model. The significant correlation between A_{type} and γ_d variables raises concerns about potential multicollinearity issues when both are included in the model. However, the introduction of a new variable representing the differences between the target and measured dry density ($\gamma_{d,diff}$) can effectively resolve this problem.

Multiple linear regression models were calibrated on the 134 observations, to identify the optimal UCS estimation model. The $Ln(UCS)$ was chosen as the ultimate functional form for the dependent variable. Table 5 presents the estimated model, which includes variables that met assumptions and exhibited both statistical and practical significance. The *F-statistic* test was used to assess the overall significance of the model with findings indicating a substantial joint impact of the model variables at a 99% confidence level (F = 695.6, p-value < .001). R^2 and R^2_{adj} were 97.48 and 97.34%, respectively. These values indicate that the independent variables accounted for over 97% of the variation in $Ln(UCS)$. The proximity of these two indicators suggests that the included variables in the model are sufficient. The low value of RMSE (i.e., 0.0913) indicates a high level of accuracy in the model's predictions. As shown in Table 5, all included variables, including some quadratic and interaction terms, are significant at the 99% confidence level (p-value < .001).

The estimated coefficient of A_{type} reveals a significant impact on *Ln(UCS)* attributable to aggregate type. Furthermore, the significant interaction between aggregate type and the H/D ratio suggests that the greatest differences in *Ln(UCS)* across aggregate types are most conspicuous at the lowest H/D ratios. The results indicate that the H/D ratio significantly influences *Ln(UCS)*. However, this effect is contingent on the H/D ratio due to a significant quadratic term, and it also varies depending on the loading mode and aggregate type, as evidenced by significant interaction terms. Although the experimental design aimed to maintain a constant dry density, minor variations were observed due to various reasons. These differences were accounted for in the model to neutralize their impact on other estimated coefficients. The findings reveal that even slight deviations in dry density have a significant effect on *Ln(UCS),* which is also influenced by the loading modality, as indicated by the significant interaction term between them. The model is in Eq. 2.

Table 4 – Correlation matrix between the variables.

	UCS	A_{type}	L_c	D	H	$R_{H/D}$	γ_d	$\gamma_{d,diff}$
UCS	1.00							
A_{type}	0.40	1.00						
L_c	-0.15	-0.04	1.00					
D	0.20	-0.00	0.03	1.00				
H	-0.73	0.02	0.02	0.21	1.00			
$R_{H/D}$	-0.80	0.02	0.00	-0.31	0.85	1.00		
γ_d	0.35	0.97	0.00	0.17	0.13	0.04	1.00	
$\gamma_{d,diff}$	-0.16	0.01	0.18	0.68	0.41	0.05	0.27	1.00

Table 5 – Estimated parameters of the *Ln*(*UCS*) model

Predictor	β-estimate	t-value	Confidence interval (95%)
A_{type}	0.682	15.78	(0.596, 0.767)
$\gamma_{d,diff}$	3.091	7.59	(2.285, 3.897)
$R_{H/D}$	-1.922	-16.35	(-2.155, -1.690)
$(R_{H/D})^2$	0.429	9.44	(-0.339, -0.519)
$A_{type} \times R_{H/D}$	-0.205	-6.03	(-0.273, 0.138)
$L_c \times R_{H/D}$	-0.256	-13.5	(-0.294, -0.219)
$L_c \times \gamma_{d,diff}$	-2.157	-4.27	(-3.156, -1.159)
constant	3.128	4.36	(2.974, 3.281)

$$Ln(UCS) = 3.128 + 0.682 \cdot A_{type} + 3.091 \cdot \gamma_{d,diff} - 1.922 \cdot R_{H/D} + 0.429 \cdot \left(R_{H/D}\right)^2 - 0.205 \cdot A_{type} - 0.256 \cdot L_c \cdot R_{H/D} - 2.157 \cdot L_c \cdot \gamma_{d,diff} \quad \textbf{eq. 2}$$

The results of Ramsey's RESET test (Ramsey, 1969) ($F_{3,123} = 2.39$, p-value = .072) indicated that the null hypothesis could not be rejected. This suggests that important variables were not omitted from the estimated model at the 95% confidence level. The Breusch-Pagan test (Breusch & Pagan, 1979) results ($\chi^2_1 = 0.95$, p-value = .330) revealed that the null hypothesis cannot be rejected, suggesting that the variance of the dependent variable does not significantly differ across various levels of the independent variable at the 95% confidence level. To assess the model's multicollinearity, the VIFs can be calculated post-model estimation. However, given the presence of significant quadratic and interaction effects, it is crucial to compute VIFs using a model estimated with the continuous independent variables centred. Table 6 shows the VIFs for the estimated model, all of which are significantly below the recommended threshold of 10. This indicates an absence of multicollinearity within the model.

Table 6 – Results of VIF multicollinearity test

Predictor	VIF
A_{type}	1.01
$\gamma_{d,diff}$	1.78
$R_{H/D}$	3.52
$(R_{H/D})^2$	1.83
$A_{type} \times R_{H/D}$	2.05
$L_c \times R_{H/D}$	2.04
$L_c \times \gamma_{d,diff}$	1.23
Mean VIF	1.92

4. DISCUSSION

4.1 Data modelling

From an analysis of linear regression output illustrated in Figure 5, we can make the following observations. First, as expected, the predicted *Ln*(*UCS*) significantly decreases as the H/D ratio increases. These results are consistent with previous studies which investigated the effects of sample size proportion on the compressive strength of cement concrete (del Viso et al., 2008; Dehestani et al., 2014; Li et al., 2018; Talaat et al., 2021. Kaufmann (1998) argued that lateral constraints induced by the stiffer loading plates at the end zones of the specimen lead to increased strength. The author inferred that this effect is more pronounced in smaller cylindrical specimens, thus explaining the higher strength of cement concrete specimens with small H/D ratios.

Figure 5 also demonstrates the influence of the different loading modes on the UCS. It is evident that the CF mode results in lower UCS values compared to the CD one. Applied stress rates in the range 8-32 kPa/s and 4-11 kPa/s were recorded for CDW specimens with 100- and 150-mm diameters, respectively. For NAT specimens, stress rates varied between 3 and 45 kPa/s for 100 mm diameter samples and between 4 and 26 kPa/s for 150-mm diameter samples. The difference in the *Ln*(*UCS*) between CF and CD loading modes is more pronounced for higher H/D ratios, suggesting a need for careful comparison of the UCS test results obtained with the two loading modes.

When comparing Figure 5-a and Figure 5-b, it is worth noting that the model (Eq. 2) consistently predicts higher *Ln*(*UCS*) values for specimens containing NAT aggregates than they do for specimens containing CDW aggregate across all the H/D ratios. This finding is consistent with existing literature that attributes higher toughness and strength values to NAT aggregates than CDW ones (Poon & Chan, 2006; Bassani & Tefa, 2018). The mechanical behaviour of CDW aggregate mixtures is significantly influenced by the type, gradation, and proportions of constituent materials in the recycled blend. Accordingly, it is advisable to limit the amount of weaker particles such as recycled clay masonry and tiles, if we wish to reduce the performance gap in terms of strength, resilient modulus and permanent deformation between virgin mixtures of the same size (Lopez-Uceda et al., 2020; Corradini et al., 2021; Lu et al., 2021). The regression model indicates that discrepancies between the actual density of specimens and the target density (MDD) have an impact on the UCS. Figure 6 depicts the evolution of the predicted *Ln*(*UCS*) as a function of the $\gamma_{d,diff}$ model variable, in which the two lines represent the CF and CD loading modes and include all the specimens, including both CDW and NAT materials. The UCS decreases as the variation between MDD and measured density increases, i.e., with a decrease in specimen density. A lower dry density indicates a higher material porosity and a weaker interlocking structure between the grains which leads to a reduction in stress support (Lade & De Boer, 1997). In the CD loading configuration, lower density results in a significant decrease in the dependent variable *Ln(UCS)* compared to the CF one.

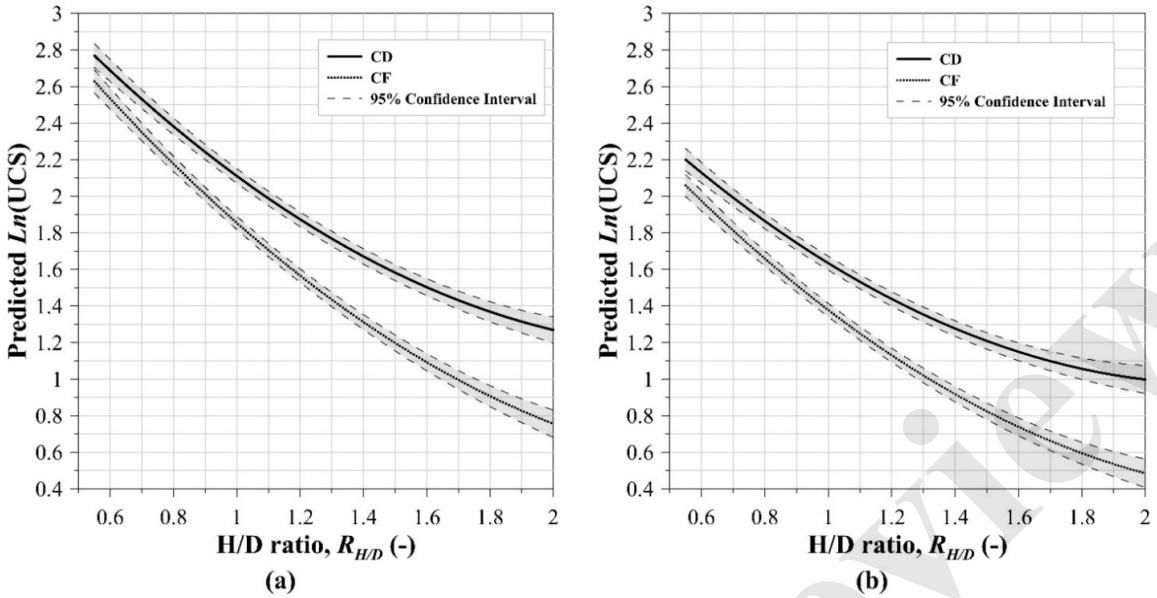

Figure 5 – Linear regression model output for (a) NAT and (b) CDW materials.

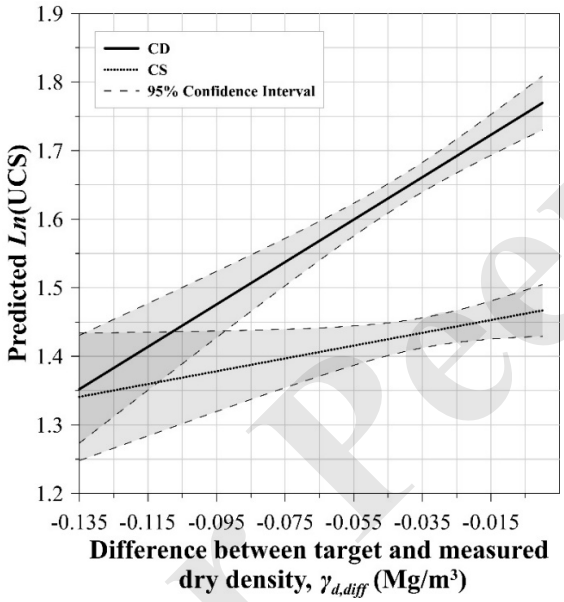

Figure 6 – Effect of the specimen's dry density on the UCS.

4.2 Conversion factors

Based on the regression model, conversion factors (denoted as *f*) have been established to facilitate the conversion of UCS values associated with a given H/D ratio into values corresponding to a different H/D ratio. These factors are given in Table 7 and Table 8 for NAT and CDW CSGMs, respectively and are differentiated for the two loading modes (CF, CD), and assuming no difference between the target and the measured dry density (i.e., posing $\gamma_{d,diff}$ equal to 0). They are valuable when comparing the UCS results achieved with samples with differing geometry or when comparing results which make reference to different codes and design specifications.

Table 7 – Conversion factors for NAT-CSGM: a) CF, b) CD loading configuration.

From H/D … \ … to H/D	0.55	0.67	0.80	1.00	1.33	1.50	1.67	2.00
0.55	1.00	0.80	0.64	0.46	0.29	0.24	0.20	0.15
0.67	1.25	1.00	0.80	0.58	0.37	0.30	0.25	0.19
0.80	1.57	1.26	1.00	0.72	0.46	0.38	0.32	0.24
1.00	2.17	1.73	1.38	1.00	0.63	0.52	0.44	0.33
1.33	3.42	2.74	2.18	1.58	1.00	0.82	0.69	0.53
1.50	4.17	3.34	2.66	1.93	1.22	1.00	0.84	0.64
1.67	4.96	3.97	3.16	2.29	1.45	1.19	1.00	0.77
2.00	6.48	5.19	4.13	2.99	1.90	1.55	1.31	1.00

(a)

From H/D … \ … to H/D	0.55	0.67	0.80	1.00	1.33	1.50	1.67	2.00
0.55	1.00	0.82	0.68	0.52	0.36	0.31	0.27	0.22
0.67	1.21	1.00	0.82	0.63	0.43	0.37	0.33	0.27
0.80	1.47	1.21	1.00	0.76	0.53	0.45	0.40	0.33
1.00	1.93	1.59	1.31	1.00	0.69	0.59	0.52	0.43
1.33	2.80	2.31	1.90	1.45	1.00	0.86	0.75	0.63
1.50	3.27	2.70	2.22	1.69	1.17	1.00	0.88	0.73
1.67	3.73	3.07	2.53	1.93	1.33	1.14	1.00	0.83
2.00	4.47	3.69	3.04	2.32	1.60	1.37	1.20	1.00

(b)

Table 8 – Conversion factors for CDW-CSGM: a) CF, b) CD loading configuration.

From H/D … \ … to H/D	0.55	0.67	0.80	1.00	1.33	1.50	1.67	2.00
0.55	1.00	0.82	0.67	0.51	0.34	0.29	0.25	0.21
0.67	1.22	1.00	0.82	0.62	0.42	0.36	0.31	0.25
0.80	1.49	1.22	1.00	0.75	0.51	0.43	0.38	0.31
1.00	1.98	1.62	1.32	1.00	0.68	0.58	0.50	0.41
1.33	2.91	2.39	1.95	1.48	1.00	0.85	0.74	0.61
1.50	3.43	2.82	2.30	1.74	1.18	1.00	0.87	0.71
1.67	3.95	3.24	2.65	2.00	1.35	1.15	1.00	0.82
2.00	4.82	3.95	3.23	2.44	1.65	1.40	1.22	1.00

(a)

From H/D … \ … to H/D	0.55	0.67	0.80	1.00	1.33	1.50	1.67	2.00
0.55	1.00	0.85	0.71	0.57	0.42	0.37	0.34	0.30
0.67	1.18	1.00	0.85	0.67	0.50	0.44	0.40	0.36
0.80	1.40	1.18	1.00	0.79	0.59	0.52	0.47	0.42
1.00	1.76	1.49	1.26	1.00	0.74	0.65	0.59	0.53
1.33	2.39	2.02	1.71	1.36	1.00	0.89	0.81	0.72
1.50	2.69	2.28	1.92	1.53	1.13	1.00	0.91	0.81
1.67	2.96	2.50	2.12	1.68	1.24	1.10	1.00	0.89
2.00	3.32	2.81	2.37	1.89	1.39	1.23	1.12	1.00

(b)

From the data reported in Table 7 and Table 8, it is evident that moving from a lower H/D ratio to a higher one entails conversion factors greater than unity. Conversely, as the H/D ratio increases, the conversion factors are below unity. For example, increasing the H/D ratio from 1.00 to 2.00 essentially reduces the USC by half, since $f = 0.33$ for NAT - CF, $f = 0.43$ for NAT - CD, $f = 0.41$ for CDW - CF, and $f = 0.53$ for CDW - CD. It is worth highlighting that the impact of the H/D ratio on UCS is less pronounced under the CD loading configuration than the CF one for both material types.

5. CONCLUSION

In the laboratory assessment of the unconfined compressive strength (UCS) of cement-stabilized granular mixtures (CSGM), several specimen geometries and loading modes are allowed in standards and technical specifications. This makes any comparisons between the strength values of different CSGMs containing natural and recycled aggregates challenging. The comparison becomes even more challenging when UCS acceptance thresholds are established for different specimen sizes in quality assurance procedures. This study

explored the effect of the H/D ratio on the UCS of two CSGM containing natural (NAT) and recycled aggregates from construction and demotion waste (CDW), respectively. Furthermore, the impact of the loading control rate of force (CF) and displacement (CD) was also investigated.

The findings of this study led to the following conclusions:

1. the UCS of the CSGMs investigated is significantly influenced by the aggregate type (NAT, CDW), specimen H/D ratio, and loading mode;
2. CSGMs containing NAT aggregates exhibited substantially higher UCS values than those containing recycled CDW material, due to the inherently weaker nature of some CDW aggregate components;
3. the increase in the H/D ratio leads to a significant reduction of the UCS, suggesting that slender specimens (i.e., greater H/D ratios) are less resistant to applied loads as already documented for cement concrete;
4. the loading mode, i.e. CF or CD, has an impact on the final UCS of CSGM; for specimens characterized by H/D ratios higher than 1.00, the CD loading configuration led to significantly greater strengths than the CF one.

A linear regression model was calibrated to quantify the effect of independent variables such as aggregate type, loading configuration, specimen size, H/D ratio, and density. The difference between the target and the effective dry density was regarded as an important parameter in the model. The regression fit metrics indicated that the calibrated model elucidates a minimum of 97% of the variability in *Ln*(UCS). This model enabled the estimation of conversion factors to facilitate a comparative analysis of UCS results across distinct specimen sizes, offering insights into the effects of varying H/D ratios while accommodating differences in material types and loading conditions.

When comparing the strength of specimens characterized by different H/D ratios, significant errors in estimation can be made, leading to inappropriate judgements of their suitability for road applications. This issue becomes paramount in the development of technical standards for the evaluation of the strength characteristics of CSGM with different aggregate sources. They must unequivocally establish the specimen's diameter and height, and the loading mode during UCS testing to avoid misleading evaluations and unsuitable comparisons. Technical specifications for quality acceptance, in which the minimum and maximum UCS thresholds are defined, need to specify the size and the loading modalities used during UCS testing. By recognising and addressing the complex effects of specimen size and loading mode, standards and specification must facilitate an accurate assessment of material properties destined for road applications.

Although slender specimens (H/D ratio equal to 2.0) may result in lower UCS values, they are always recommended due to their experimental advantages, i.e., (i) mitigating the confinement effect generated by the loading plates and (ii) avoiding inconsistent failure modes characterized by diagonal or side fractures due to shear actions. In the case of different sample sizes and/or loading modes, the technical standards for the assessment of CSGM, i.e., the EN 13286-41 (European Committee for Standardization, 2021) and EN 14227-1

(European Committee for Standardization, 2013b), should include conversion factors derived from observing the effects of experimental variables on the considered strength parameter. This experimental investigation helped to address the gap in knowledge that exists when the same regulations allow the use of different sample geometries and testing procedures.

The validity of the results presented here are limited to specimens ranging in height from 55 to 200 mm and diameter size from 100 to 150 mm with a limited maximum aggregate size of 20 mm. Aggregates containing larger particles can only be tested by increasing the specimen size. However, the current practise is to evaluate strength on small to medium-sized specimens, which need small and easily manageable volumes of material in testing laboratories for both product development research and quality assessment in accordance with technical specifications.

In terms of the aggregate, all specimens had the same particle size distribution to limit the number of variables and ensure greater experimental control. Further studies will provide insights into the effects of testing independent factors on the UCS of CSGM with different particle size distributions. Similarly, the results are limited to the type and composition of the CDW recycled aggregate considered here. CDW materials with a different composition (e.g., containing only crashed concrete particles) could provide different results.

ACKNOWLEDGEMENTS

The authors would like to thank Mr. Alessandro Gancitano and Ms. Eleonora Mariotti for their support with part of this research activity. The natural aggregates and recycled aggregates were provided by Spinelli & Mannocchi S.r.l. and Cavit S.p.A. respectively, while the cement was provided by Italcementi S.p.A., all of whom are gratefully acknowledged for their support.

DISCLOSURE STATEMENT

The authors report there are no competing interests to declare.

REFERENCES

American Society for Testing and Materials. (2007). *Standard Test Methods for Compressive Strength of Molded Soil-Cement Cylinders* (ASTM D1633-07). ASTM International.

American Society for Testing and Materials. (2009). *Unconfined Compressive Strength of Compacted Soil-Lime Mixtures* (ASTM D5102-09). ASTM International.

American Society for Testing and Materials. (2012). *Standard Test Methods for Laboratory Compaction Characteristics of Soil Using Standard Effort (12,400 ft-lbf/ft3 (600 kN-m/m3))* (ASTM D698-12). ASTM International.

Applied Research Associates Inc. (2004). *Guide for Mechanistic-Empirical Design of New and Rehabilitated Pavement Structures* (Final Report NCHRP Project 1-37A). Transportation Research Board, National Research Council.

Autelitano, F., & Giuliani, F. (2016). Electric arc furnace slags in cement-treated materials for road construction: Mechanical and durability properties. *Construction and Building Materials*, *113*, 280–289. https://doi.org/10.1016/j.conbuildmat.2016.03.054

Bassani, M., Riviera, P. P., & Tefa, L. (2017). Short-Term and Long-Term Effects of Cement Kiln Dust Stabilization of Construction and Demolition Waste. *Journal of Materials in Civil Engineering*, *29*(5), 04016286. https://doi.org/10.1061/(ASCE)MT.1943-5533.0001797

Bassani, M., & Tefa, L. (2018). Compaction and freeze-thaw degradation assessment of recycled aggregates from unseparated construction and demolition waste. *Construction and Building Materials*, *160*, 180–195. https://doi.org/10.1016/j.conbuildmat.2017.11.052

Bassani, M., Tefa, L., Russo, A., & Palmero, P. (2019). Alkali-activation of recycled construction and demolition waste aggregate with no added binder. *Construction and Building Materials*, *205*, 398–413. https://doi.org/10.1016/j.conbuildmat.2019.02.031

Biswal, D. R., Sahoo, U. C., & Dash, S. R. (2020). Mechanical characteristics of cement stabilised granular lateritic soils for use as structural layer of pavement. *Road Materials and Pavement Design*, *21*(5), 1201–1223. https://doi.org/10.1080/14680629.2018.1545687

Breusch, T. S., & Pagan, A. R. (1979). A Simple Test for Heteroscedasticity and Random Coefficient Variation. *Econometrica*, *47*(5), 1287–1294. https://doi.org/10.2307/1911963

Centro Sperimentale Interuniversitario di Ricerca Stradale. (2001). *Studio a carattere pre-normativo delle norme tecniche di tipo prestazionale per capitolati speciali d'appalto*. Ministero delle Infrastrutture e dei Trasporti.

Corradini, A., Cerni, G., & Porceddu, P. R. (2021). Comparative study on resilient modulus of natural and post-quake recycled aggregates in bound and unbound pavement subbase applications. *Construction and Building Materials*, *297*, 123717. https://doi.org/10.1016/j.conbuildmat.2021.123717

Dehestani, M., Nikbin, I. M., & Asadollahi, S. (2014). Effects of specimen shape and size on the compressive strength of self-consolidating concrete (SCC). *Construction and Building Materials*, *66*, 685–691. https://doi.org/10.1016/j.conbuildmat.2014.06.008

del Viso, J. R., Carmona, J. R., & Ruiz, G. (2008). Shape and size effects on the compressive strength of high-strength concrete. *Cement and Concrete Research*, *38*(3), 386–395. https://doi.org/10.1016/j.cemconres.2007.09.020

Department of the Army & Department of the Air Force. (1994). *Pavement design for roads, streets, and open storage areas, elastic layered method* (Technical Manual TM 5-822-13/AFJMAN 32-1018).

Esfahani, M. A. (2020). Evaluating the feasibility, usability, and strength of recycled construction and demolition waste in base and subbase courses. *Road Materials and Pavement Design*, *21*(1), 156–178. https://doi.org/10.1080/14680629.2018.1483259

European Committee for Standardization. (2004a). *Unbound and hydraulically bound mixtures. Method for the manufacture of test specimens of hydraulically bound mixtures using vibrating hammer compaction* (EN 13286-51). European Committee for Standardization.

European Committee for Standardization. (2004b). *Unbound and hydraulically bound mixtures. Method for the manufacture of test specimens of hydraulically bound mixtures using vibrocompression* (EN 13286-52). European Committee for Standardization.

European Committee for Standardization. (2004c). *Unbound and hydraulically bound mixtures. Methods for the manufacture of test specimens of hydraulically bound mixtures using axial compression* (EN 13286-53). European Committee for Standardization.

European Committee for Standardization. (2004d). *Unbound and hydraulically bound mixtures—Method for the manufacture of test specimens of hydraulically bound mixtures using Proctor equipment or vibrating table compaction* (EN 13286-50). European Committee for Standardization.

European Committee for Standardization. (2009). *Tests for geometrical properties of aggregates. Part 11: Classification test for the constituents of coarse recycled aggregate* (EN 933-11). European Committee for Standardization.

European Committee for Standardization. (2010). *Unbound and hydraulically bound mixtures—Part 2: Test methods for laboratory reference density and water content—Proctor compaction* (EN 13286-2). European Committee for Standardization.

European Committee for Standardization. (2011). *Cement—Part 1: Composition, specifications and conformity criteria for common cements* (EN 197-1). European Committee for Standardization.

European Committee for Standardization. (2013a). *Tests for mechanical and physical properties of aggregates—Part 6: Determination of particle density and water absorption* (EN 1097-6:2013).

European Committee for Standardization. (2013b). *Unbound and hydraulically bound mixtures—Part 1: Specifications for cement bound granular mixtures* (EN 14227-1). European Committee for Standardization.

European Committee for Standardization. (2021). *Unbound and hydraulically bound mixtures—Part 41: Test method for the determination of the compressive strength of hydraulically bound mixtures* (EN 13286-41). European Committee for Standardization.

Federal Highway Administration Research and Technology. (2016). *User Guidelines for Waste and Byproduct Materials in Pavement Construction* (Final Report FHWA-RD-97-148). U.S. Department of Transportation, Federal Highway Administration. https://www.fhwa.dot.gov/publications/research/infrastructure/structures/97148/toc.cfm

Halsted, G. E., Luhr, D. R., & Adaska, W. S. (2006). *Guide to Cement-Treated Base*. Portland Cement Association.

James, G., Witten, D., Hastie, T., & Tibshirani, R. (2021). *An Introduction to Statistical Learning: With Applications in R*. Springer US. https://doi.org/10.1007/978-1-0716-1418-1

Kaufmann, W. (1998). *Strength and Deformations of Structural Concrete Subjected to In-Plane Shear and Normal Forces*. Birkhäuser. https://doi.org/10.1007/978-3-0348-7612-4

Lade, P. V., & De Boer, R. (1997). The concept of effective stress for soil, concrete and rock. *Géotechnique*, *47*(1), 61–78. https://doi.org/10.1680/geot.1997.47.1.61

Li, M., Hao, H., Shi, Y., & Hao, Y. (2018). Specimen shape and size effects on the concrete compressive strength under static and dynamic tests. *Construction and Building Materials*, *161*, 84–93. https://doi.org/10.1016/j.conbuildmat.2017.11.069

Lopez-Uceda, A., Ayuso, J., Jiménez, J. R., Galvín, A. P., & Del Rey, I. (2020). Feasibility study of roller compacted concrete with recycled aggregates as base layer for light-traffic roads. *Road Materials and Pavement Design*, *21*(1), 276–288. https://doi.org/10.1080/14680629.2018.1483257

Lotfi, H. A.-L., & Witczak, M. W. (1981). Dynamic characterization of cement-treated base/subbase materials. *Transportation Research Record*, *1031*.

Lu, C., Chen, J., Gu, C., Wang, J., Cai, Y., Zhang, T., & lin, G. (2021). Resilient and permanent deformation behaviors of construction and demolition wastes in unbound pavement base and subbase applications. *Transportation Geotechnics*, *28*, 100541. https://doi.org/10.1016/j.trgeo.2021.100541

Maher, M. H., & Ho, Y. C. (1993). Behavior of Fiber-Reinforced Cemented Sand Under Static and Cyclic Loads. *Geotechnical Testing Journal*, *16*(3), 330–338. https://doi.org/10.1520/GTJ10054J

Mohammad, L. N., Raghavandra, A., & Huang, B. (2000). Laboratory Performance Evaluation of Cement-Stabilized Soil Base Mixtures. *Transportation Research Record*, *1721*(1), 19–28. https://doi.org/10.3141/1721-03

Mohammadinia, A., Arulrajah, A., Sanjayan, J., Disfani, M. M., Bo, M. W., & Darmawan, S. (2014). Laboratory Evaluation of the Use of Cement-Treated Construction and Demolition Materials in Pavement Base and Subbase Applications. *Journal of Materials in Civil Engineering*, *27*(6), 04014186. https://doi.org/10.1061/(ASCE)MT.1943-5533.0001148

Olard, F., & Perraton, D. (2010). On the Optimization of the Aggregate Packing Characteristics for the Design of High-Performance Asphalt Concretes. *Road Materials and Pavement Design*, *11*(sup1), 145–169. https://doi.org/10.1080/14680629.2010.9690330

Poon, C. S., & Chan, D. (2006). Feasible use of recycled concrete aggregates and crushed clay brick as unbound road sub-base. *Construction and Building Materials*, *20*(8), 578–585. https://doi.org/10.1016/j.conbuildmat.2005.01.045

Ramsey, J. B. (1969). Tests for Specification Errors in Classical Linear Least-Squares Regression Analysis. *Journal of the Royal Statistical Society: Series B (Methodological)*, *31*(2), 350–371. https://doi.org/10.1111/j.2517-6161.1969.tb00796.x

Rashidi, M., & Ashtiani, R. S. (2019). *Scale Effects in the Indirect Tensile and Unconfined Compressive Strength Tests of Cement-Stabilized Base Materials*. 628–639. https://doi.org/10.1061/9780784482124.064

StataCorp. (2021). *Stata Statistical Software* (Release 17) [Computer software]. StataCorp LLC.

Talaat, A., Emad, A., Tarek, A., Masbouba, M., Essam, A., & Kohail, M. (2021). Factors affecting the results of concrete compression testing: A review. *Ain Shams Engineering Journal*, *12*(1), 205–221. https://doi.org/10.1016/j.asej.2020.07.015

Tataranni, P., Sangiorgi, C., Simone, A., Vignali, V., Lantieri, C., & Dondi, G. (2018). A laboratory and field study on 100% Recycled Cement Bound Mixture for base layers. *International Journal of Pavement Research and Technology*, *11*(5), 427–434. https://doi.org/10.1016/j.ijprt.2017.11.005

The British Standards Institution. (2018). *Hydraulically bound and stabilized materials for civil engineering purposes—Part 2: Sample preparation and testing of materials during and after treatment* (BS 1924-2:2018). BSI Standards Limited.

Wang, N., Chen, F., Ma, T., Luan, Y., & Zhu, J. (2022). Compaction performance of cold recycled asphalt mixture using SmartRock sensor. *Automation in Construction*, *140*, 104377. https://doi.org/10.1016/j.autcon.2022.104377

Wang, Y., Zhang, J., Wang, X., & Zhang, Z. (2020). Laboratory Investigation on the Performance of Cement Stabilized Recycled Aggregate with the Vibration Mixing Process. *Mathematical Problems in Engineering*, *2020*, e6625370. https://doi.org/10.1155/2020/6625370

Wooldridge, J. M. (2019). *Introductory Econometrics: A Modern Approach* (7th edition). Cengage Learning.

Xuan, D. X., Houben, L. J. M., Molenaar, A. A. A., & Shui, Z. H. (2012). Mechanical properties of cement-treated aggregate material – A review. *Materials & Design*, *33*, 496–502. https://doi.org/10.1016/j.matdes.2011.04.055

Xue, X., Gao, J., & Hu, K. (2022). Performance Evaluation of Cement Stabilized Mixture with Recycled Aggregate from Construction and Demolition Waste. *Iranian Journal of Science and Technology, Transactions of Civil Engineering*, *46*(4), 3093–3106. https://doi.org/10.1007/s40996-021-00739-z

Yoder, E. J., & Witczak, M. W. (1975). *Principles of Pavement Design*. John Wiley & Sons.